Draft version August 3, 2017
Preprint typeset using LaTeX style emulateapj v. 12/16/11

MODAL NOISE MITIGATION THROUGH FIBER AGITATION FOR FIBER-FED RADIAL VELOCITY SPECTROGRAPHS

Ryan Petersburg, Tyler McCracken, Dominic Eggerman, Debra Fischer
Department of Astronomy, Yale University, 52 Hillhouse Ave, New Haven, CT 06511, USA; ryan.petersburg@yale.edu
Draft version August 3, 2017

ABSTRACT

Optical fiber modal noise is a critically limiting factor for high precision spectroscopy signal-to-noise in the near-infrared and visible. Unabated, especially for highly coherent light sources, modal noise can induce radial velocity errors that hinder the discovery of low-mass (and potentially earth-like) planets. Previous research in this field has found sufficient modal noise mitigation through use of an integrating sphere, but this requires extremely bright light sources, a luxury not necessarily afforded calibration for the next-generation of high resolution optical-range spectrographs. Otherwise, mechanical agitation, which "mixes" the fiber's modal patterns and allows the noise to be averaged over minutes-long exposures, provides some noise reduction but the methods have not been fully optimized by the community. Therefore, we have filled out the parameter space of modal noise agitation techniques in order to better understand agitation's contribution to mitigating modal noise and to discover the optimal strategy for agitating fibers. We found that modal noise was best suppressed by the chaotic nature of coupled harmonic motion at high amplitude for fibers with large core diameters and low azimuthal symmetry, reducing modal noise induced radial velocity error to below 10 cm/s. This work has subsequently influenced the design of a fiber agitator to be installed with the Extreme Precision Spectrograph.

1. INTRODUCTION

Radial velocity (RV) exoplanet detection has continually been on the path of discovering less massive planets. The current goal of RV spectroscopy is $10\,\mathrm{cm\,s^{-1}}$ precision, thereby allowing the discovery of earth-like planets orbiting G and K stars in their respective habitable zone (Fischer et al. 2016). Therefore, the next-generation of visible-band RV spectrographs, such as the Extreme Precision Spectrograph (EXPRES, (Jurgenson et al. 2016)) and ESPRESSO [GET MEGEVAND ET AL 2012 CITATION], require precision engineering and extreme stability to yield such results.

Multi-mode fibers have become the backbone of such RV spectrograph design. An essential link between the telescope focus and the spectrograph optics, optical fibers isolate the spectrograph from vibrational and thermal noise. Optical fibers also provide spatial scrambling to stellar light since the spatial distribution of a fiber output is, for the most part, independent of the input [CITATION NEEDED]. This effect has been amplified through the use of double scramblers [CITATION NEEDED] and non-circular fiber core cross-sectional shapes including octagons and rectangles [CITATION NEEDED].

Optical fibers also transmit light from calibration sources–such as wavelength calibrators and broadband flat-field sources–into the spectrograph. Laser frequency combs, especially the recently deployed astrocomb [CITATION NEEDED], produce thousands of evenly spaced highly-coherent emission lines over a wide frequency range. When these narrow-emission lines propagate through a multi-mode fiber, they create [BETTER WORD???] noise that limits the signal-to-noise ratio (SNR) of the instrument and potentially induces false signals into the data. This noise is caused by interference between the finite number of electromagnetic modes that can propagate along a multi-mode fiber, and has therefore been coined *modal noise*.

Some next-generation RV spectrographs [CITATIONS NEEDED, e.g. iLocator] have moved to a completely single-mode fiber architecture to help alleviate these complications. As apparent in their name, single-mode fibers only propagate a single electromagnetic mode and are therefore free from any modal noise. Due to the small core-size of single-mode fibers, however, coupling light from the telescope into these fibers is challenging, requiring robust adaptive optics that have not yet been fully developed. Additionally, single-mode fibers have a very limited bandwidth over which they propagate a single-mode. Therefore, these fibers may not be truly single-mode across the full band of wavelength calibration meaning the optical design requires multiple band-depend paths. Finally, Halverson et al. (2015) asserts that a type of polarization "modal noise" exists in single mode fibers. Thus, the study of modal noise reduction methods may still be necessary even for these novel single-mode-fiber injected instruments.

In this paper, we attempt to discern the optimal strategy for reducing modal noise in multi-mode fibers propagating coherent visible light through mechanical agitation. We begin by defining modal noise and exploring how previous experiments have mitigated it through static and dynamic methods (section 2). We then describe our own methods of fiber agitation (section 3) and discuss results from using these methods on fibers of varying cross-sectional shapes and coupling permutations (section 4). Finally, we relate these results to limits in RV precision (section 5) and discuss how these results should be applied to next-generation RV spectrographs (section 6). The work in this paper was conducted to influence design decisions for EXPRES.

2. OPTICAL FIBER MODAL NOISE

Light propagates through an optical fiber in an integer number of electromagnetic modes. The exact calculation for this value is non-trivial since it depends on the instantaneous fiber geometry, injection parameters, and many other variables. The maximum number of modes for a step-index circular cross-section fiber is approximately given by

$$M_{circ} \approx \frac{4}{\pi^2} V^2 \tag{1}$$

where V is the normalized frequency of the fiber given as

$$V = \left(\frac{2\pi r \mathrm{NA}}{\lambda} \right)^2 . \tag{2}$$

$\mathrm{NA} = \sqrt{n_{core}^2 - n_{clad}^2}$ is the numerical aperture of the fiber determined by the core (n_{core}) and cladding (n_{clad}) indices of refraction, r is the core radius, and λ is the wavelength of propagated light. This approximation is more difficult for a rectangular fiber, but Nikitin et al. (2011) shows empirically using electromagnetic and geometrical arguments that

$$\frac{M_{rect}}{M_{circ}} \propto \frac{ab}{r^2} \tag{3}$$

where a and b are the side lengths of the rectangular cross-section. Therefore, we will assert more generally that

$$M \propto A \left(\frac{\mathrm{NA}}{\lambda} \right)^2 \tag{4}$$

where A is the cross-sectional area of the fiber regardless of shape.

When coherent light is propagated through a multimode fiber, a high contrast speckle pattern known as modal noise is produced at the output for both the near-field (fiber face) and far-field (a few what's his nuts name lengths), figure 1. Modal noise is an inherent property of all multi-mode fibers regardless of the cross-sectional core shape (Sablowski et al. 2015) [OTHER CITATIONS?] and arises from light coupling from mode-to-mode as it propagates through fiber, causing slight variances in the path length travelled and producing the observered interference pattern. For RV spectrographs this causes two problems: 1) it limits the maximum signal-to-noise ratio and 2) systematic variations in the speckle pattern will mask themselves as minute shifts on the focal plane causing errant RV signatures.

2.1. *Limits on SNR*

Due to its high contrast, modal noise can severely decrease the signal-to-noise ratio of an RV spectrograph (Epworth 1978; Baudrand & Walker 2001; Lemke et al. 2011). Additionally, if the speckle pattern drifts between exposures, especially with some period of motion, modal noise can cause errant RV signatures in the data that is distinct from errors due to poor scrambling (Mahadevan et al. 2014).

Modal noise's dependence on static physical properties of optical fibers is well documented. Modal noise SNR is increased for larger fiber core diameters (Sablowski et al. 2015) [CITE OTHERS HERE] and for non-circular fibers

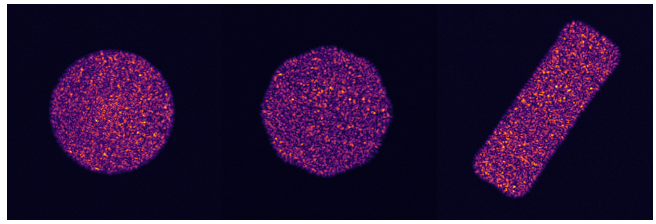

Fig. 1.— Examples of unmitigated modal noise for a rectangular (left), octagonal (middle), and circular (right) optical fiber. All three fibers shown here have approximately the same cross-sectional area, meaning that they each are propagating about the same number of electromagnetic modes (see section 3).

over circular fibers (Stürmer et al. 2016; Sablowski et al. 2015) [CITE OTHERS HERE]. Increasing the number of static bends in a fiber slightly increases SNR (Imai & Asakura 1979). Far field modal noise SNR is strongly anti-correlated with injected focal ratio (Sablowski et al. 2015), while the near field modal noise SNR is independent of injected focal ratio (Baudrand & Walker 2001). Finally, modal noise SNR was shown to be anti-correlated with wavelength (see equation 1), poorly responsive to input pupil obstructions, and independent of fiber length greater than a few meters (Baudrand & Walker 2001).

2.2. *Dynamic variations*

Modal noise is also affected by dynamic optical properties, meaning it can induce false RV's on the spectrograph, in addition to being an issue of SNR. The speckle pattern is primarily wavelength dependent as theoretically explained in section 3. However, next-generation RV spectrographs are using stable wavelength calibrators rendering this problem effectively irrelevant. Otherwise, the speckle pattern seen at the end of a fiber shifts over time due to many reasons, but most commonly because of (Epworth 1978):

1. Temperature variation
2. Fiber input illumination variation
3. Fiber movement (bending, twisting, etc.)

These three conditions inevitably pose problems when imaging a spectrum since they are inherent to modern fiber-fed RV spectrographs (Baudrand & Walker 2001; Mahadevan et al. 2014).

The resultant RV shift (ΔRV) due to a shifting speckle pattern centroid at the end of a fiber is calculated in a similar manner to scrambling gain [CITATION]:

$$\Delta RV = \frac{c}{R} \frac{\Delta d}{D} \tag{5}$$

where c is the speed of light in a vacuum, R is the resolution of the spectrograph, Δd is the shift in the centroid of the fiber in the dispersion direction and D is the slit width (or short-end length of a rectangular fiber). Notice that for a $R = 150,000$ spectrograph fed by a 33 µm slit attempting to reach 1 m s^{-1} RV precision per wavelength calibration line, the required stability of the centroid along the dispersion direction is 0.165 µm.

Modal noise can be reduced by continuously exacerbating one of the above three causes of drift, thereby shifting the speckle pattern throughout an appropriately long camera exposure and averaging out the noise. Controlled temperature variation (option 1) is non-ideal because a 1 meter fiber requires approximately 8°C fluctuations to visibly decorrelate the speckle pattern (Redding et al. 2013) [MORE CITATIONS???], but the spectrograph environment is supposed to remain thermally stable for higher precision [CITATION???]. Therefore, RV spectrographs have been left with either varying the illumination (option 2) or shaking the fiber (option 3).

As summarized in table 1, modal noise reduction techniques have been discussed by many experiments concerned with RV spectroscopy. The majority deal with some form of agitation that physically changes the position of the fiber (mechanical agitation) while Mahadevan et al. (2014) and Halverson et al. (2014) explored the effectiveness of varying the illumination of the fiber face. The variation in frequency and amplitude for the mechanical agitation methods is unfortunately quite wide and connections are difficult to make. However, there have been slight trends in the results and the discussed assumptions so far are as follows:

- The frequency of agitation should be greater than $1/\tau$, where τ is the exposure time (Baudrand & Walker 2001)
- Noise is more effectively reduced by high amplitude motion (Lemke et al. 2011; McCoy et al. 2012)
- Higher frequencies (with an upper limit) show further noise reduction (Lemke et al. 2011)
- Adding a high frequency "tweeter" to a large amplitude "woofer" reduces noise further (Plavchan et al. 2013)
- Hand agitation is better than any form of mechanical agitation (Lemke et al. 2011; McCoy et al. 2012; Mahadevan et al. 2014; Roy et al. 2014)

Although this has been good for subjective intuition, the exact mechanisms behind the improvements in SNR and prevention of RV drift have not been explored.

Varying the input illumination of a fiber using an integrating sphere, diffuser, and rotating mirror showed gradual improvements in modal noise reduction due to the addition of further illumination variation. However, the integrating sphere, an integral part of these methods, has a throughput efficiency of approximately 10^{-6} and is not feasible to be introduced in the science light optical path. To allow flexible observing programs, iėšcience observations bracketed by precision wavelength calibraiton sources, the modal noise mitigation technique needs to be efficient.

In the following sections, we fill out the parameter space of fiber agitation methods to a greater extent than previous studies. We are interested in seeing trends across different amplitudes, frequencies, fiber shapes/sizes, and coupling permutations to make more precise conclusions about the nature of modal noise mitigation through fiber agitation.

3. EXPERIMENTAL SETUP

The number of modes a fiber supports is largely determined by its cross-sectional area. For tesing and characterizting agitation methods across multiple firber geometries, we chose a fibers with similar cross-sectional areas. Table 2 lists the fibers used in our experiment. Notice that the 200 µm circular, 200 µm octagonal, and 100 µm × 300 µm rectangular fiber all have approximately the same cross-sectional area, meaning they can each support a similar number of modes.

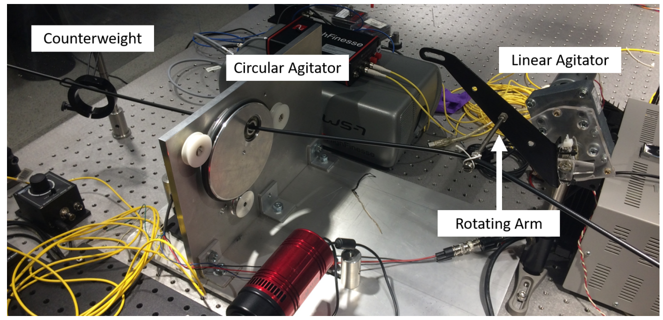

Fig. 2.— Linear and circular agitator used in these modal noise tests. The linear agitator rotates along the length of the fiber while the circular agitator rotates perpendicular to it. The counterweight was included to confirm that the fiber would always be taught between the two agitators, preventing it from over-bending or bunching up.

Two different methods of mechanical agitation are used: the first produces a linear type motion in which the fiber is moved up and down, the other is a circular type motion in which the fiber cross section is rotated perpendicular to direction of propagation. The linear agitation has variable amplitude allowing for 80-320 mm agitation amplitudes at 80 mm intervals and a variable frequency in the range of 0.03 to 1.0 Hz. For the circular agitator, the fiber is rotated in circular path with a set radius of 80 mm **is this correct?** at a variable frequency of 0.1 to 1.5 Hz. Routing a fiber through both agitators produces what we call "coupled agitation". Both agitators are shown in figure 2, frequencies are independently set by adjusting the appropriate DC-motor drive volatge. The amplitude of the linear agitator is set by the position of the lifting arm **label lift arm** and a small counterweight is present to keep a minimal amount of tension in the fiber and prevent it from **flying about?!?**.

All image data was collected with the Fiber Characterization Station (FCS, figure 3), a multipurpose device that is able to simultaneously image the input face, output face (or near field), and output pupil (or far field) of the fiber under test. Specifications for the FCS cameras are listed in table 3.

Expnad on this

Images exposure times are set according to the frequency of agitation such that each exposure lasts exactly one period of rotation. For example, if an agitator is set to rotate at 0.5 Hz, each image will be exposed for 2 s. We do this to confirm that only one full rotation is being recorded and allow for "number of rotations" to be another parameter for exploration.

For each data set, we take a sequence of ten exposures in order to:

1. reduce statistical errors in our SNR calculations potentially caused by camera noise or small problems with our agitators
2. observe the effects of agitation at longer exposures time by co-adding multiple single-rotation images

TABLE 1
Previous study of dynamic modal noise mitigation methods

Reference	Method	Frequency	Amplitude
Daino et al. (1980)	Loudspeaker	110 Hz	"Sufficient"
Baudrand & Walker (2001)	—	30 Hz	1 mm
Lemke et al. (2011)	Loudspeaker	1.5 Hz	—
	Loudspeaker	80 Hz	—
McCoy et al. (2012)	Paint mixer	60 Hz	—
	Hand agitated	1-2 Hz	10-15 cm
	Mechanical agitator	"Low"	"High"
Plavchan et al. (2013)	"Tweeter"	100 Hz	1 mm
	"Woofer"	1 Hz	25 mm
Mahadevan et al. (2014)	Int. Sph. + Diff.	—	—
	McCoy agitator	"Low"	"High'
	Hand agitation	1-2 Hz	10 cm
Halverson et al. (2014)	Int. Sph. + Diff.	—	—
	Int. Sph. + OAP	—	—
Roy et al. (2014)	Rail agitator	"Low"	"High"
Sablowski et al. (2015)	Mechanical "Excenter"	2 Hz	20 cm

TABLE 2
Tested optical fibers. All fibers have NA = 0.22.

Shape	Size	Manufacturer
Circular	100 µm	Polymicro
Circular	200 µm	Polymicro
Circular	600 µm	Thorlabs
Octagonal	100 µm	CeramOptec
Octagonal	200 µm	CeramOptec
Rectangular	100 µm × 300 µm	CeramOptec

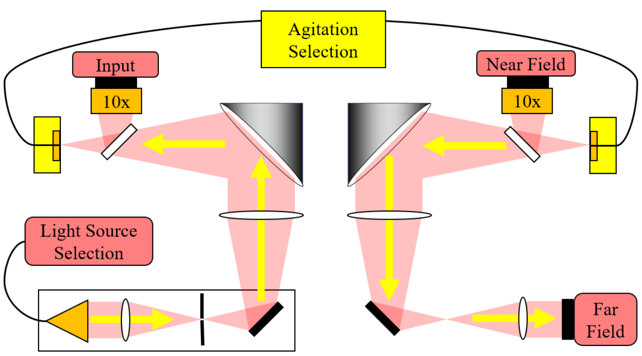

Fig. 3.— Schematic of the Fiber Characterization Station. Light from either a single-mode fiber-fed 652 nm Toptica diode laser or from a selection of Thorlabs mounted LEDs fed by a 100 µm circular fiber is fed into the station in the bottom left. This light is spatially filtered, collimated, and injected into the test fiber. The injection face of the test fiber is imaged at 10x magnification by the input camera to allow for precision alignment. Light propagates through the test fiber and our choice of agitator mixes the modes. Light is then ejected from the test fiber and split between the 10x magnified near field camera and the far field camera.

TABLE 3
Fiber Characterization Station imaging specifications

Name	Camera	Pixel Size	Magnification
Input	Atik 450	3.45 µm	10
Near Field	Atik 450	3.45 µm	10
Far Field	Atik 383L+	5.4 µm	N/A

together.

Whenever collecting images sets to be compared, we also take a set of images with the agitator turned off (hereafter called *unagitated images*) and a set of images using a broadband LED light source. This allows for direct comparison to a worst-case and best-case scenario respectively.

Each data set is comprised of a 10 exposures each of the following cases:

1. the fiber being actively agitated
2. the fiber routed through the agitator but without agitation
3. the unagitated fiber illuminated with a broadband LED.

Multiple images are taken to reduce statistical errors in our SNR calculations potentially caused by camera noise or small problems with our agitators and to observe the effects of agitation at longer exposures time by co-adding multiple single-rotation images together. The LED source acts as a best-case scenario and the unagitated as a worst case.

We quantify modal noise using the SNR of light within the fiber face of a near field image calculated as

$$\mathrm{SNR} = \frac{\mathrm{median}(I_{filt})}{\mathrm{stdev}(I_0 - I_{filt})} \tag{6}$$

where I_0, the original raw image, is heavily median filtered to produce I_{filt}. The typical SNR (where the "signal" is assumed to be a top-hat function across the fiber face) could not be used due to slight intensity-varying diffraction effects across the near field image. Subtracting I_{filt} from I_0 therefore produces a noise pattern that reflects the modal noise and not these large-scale diffraction-caused variances. We use a circular 51-pixel median filter rather than a low-order polynomial or Gaussian fit because these functions could not sufficiently fit the raw fiber images. The size of the filter kernel was chosen such that speckles on unagitated images were sufficiently filtered without removing structure from the edges of the fibers. The numerator in equation 6 is calculated as the median (rather than the mean, for example) of I_{filt} to prevent dust on the fiber face or optics from skewing this value.

We calculate the SNR for each individual image and average them together within each data set to yield a single-rotation SNR. We then co-add images 1-2, 1-3, 1-4, ..., 1-10 and calculate the SNR for each case. The SNR for images 1-10 is presented as the ten-rotation SNR and each intermediate step as two-rotation SNR, three-rotation SNR, etc.

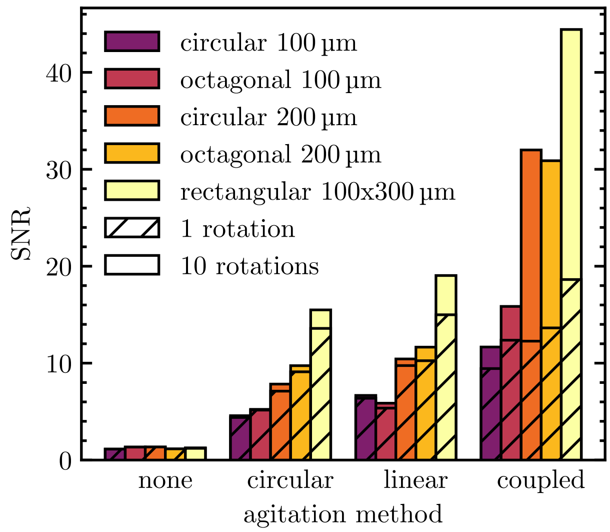

Fig. 4.— SNR comparison for varying fiber geometries and agitation methods. SNR for 10 rotation images was calculated after co-adding ten single rotation images.

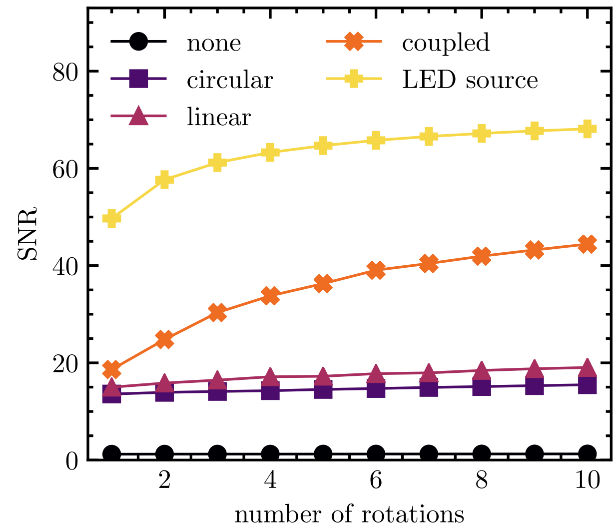

Fig. 5.— SNR for the 100x300 µm rectangular fiber using various agitation methods. The SNR is calculated after co-adding the 1 rotation images.

Far field images are taken for each data set and analyzed using the maximum intensity rather than the median intensity as the numerator in equation 6. The far field speckle pattern is of interest in precision RV spectroscopy as it is what illuminates the optics. However, mapping the far field speckle pattern to RV error would require numerical simulations with the optical design software and is out of the scope of this paper. That being said, all results listed in the following section may be extended to the far field though we omit this data for conciseness.

4. RESULTS

4.1. *Method of Agitation and Fiber Geometry*

We compare the two individual agitation methods and coupled agitation using all of the fibers previously listed in table 2. The linear agitator was set to an amplitude of (80 mm) and the frequency of both agitators to (1.0 Hz, all images are taken with 1 s exposures.

Results for the single-rotation and ten-rotation cases are shown in figure 4. Across all fiber shapes and sizes and number of rotations, the linear agitator appears to be slightly better than the circular agitator. There is a similar increase in SNR when looking at coupled agitation in single-rotations. However, coupling the agitation over ten-rotations significantly increases the SNR for all fiber configurations.

To better understand why coupled agitation is so effective at reducing modal noise at longer exposures, we also analyze the effect of each agitation method over multiple rotations, as shown in figure 5 for the 100 µm × 300 µm rectangular fiber. SNR shows continued improvement beyond a single rotation when coupling the agitation methods at a similar rate to when the fiber is lit by an LED, a broadband source. Circular and linear agitation, however, are effectively plateaued after the first rotation.

4.2. *Adding a tweeter*

4.3. *Amplitude and Frequency of Agitation*

TABLE 4
Fiber assemblies tested for the fiber coupling experiment

Test	1st Fiber	2nd Fiber
1	Circular 200 µm	Circular 200 µm
2	Circular 100 µm	Circular 200 µm
3	Octagonal 200 µm	Circular 200 µm

We use the 100 µm × 300 µm rectangular fiber and the two agitators separately to test the effects of agitation amplitude and frequency of rotation on the SNR. We can only test amplitude on the linear agitator and take an image set for each position on the rotating arms. We test frequency on each of the linear and circular agitators at approximately equally spaced frequencies across their entire frequency range.

Results from these tests are shown in figure 6. There is a strong position correlation between linear agitation amplitude using both the single-rotation and ten-rotation analyses. There also appears to be a slight increase in SNR for the linear agitator at higher frequencies after ten rotations, however there is no such increase for the single-rotations or any of the frequencies when using the circular agitator.

4.4. *Fiber Coupling*

It is not uncommon for RV spectrographs to have multiple fiber links for carrying calibration and/or science light from the source (lamp or telescope respectively) to the spectrograph and ultimately detector. This results in having to couple light from one fiber to another and begs the question, is there a prefered fiber to agitate or must we agitate as many as possible? Agitating the first fiber in a multi-fiber system serves to vary the input illumination of subsequent fibers, similar to the integrating sphere proposed by mahadevan and halversion. To study the effects of such an architecture, we agitated individual fibers in a multi-fiber assembly where each fiber could have different core sizes and shape. We test three distinct cases outlined in table 4 and compare them against

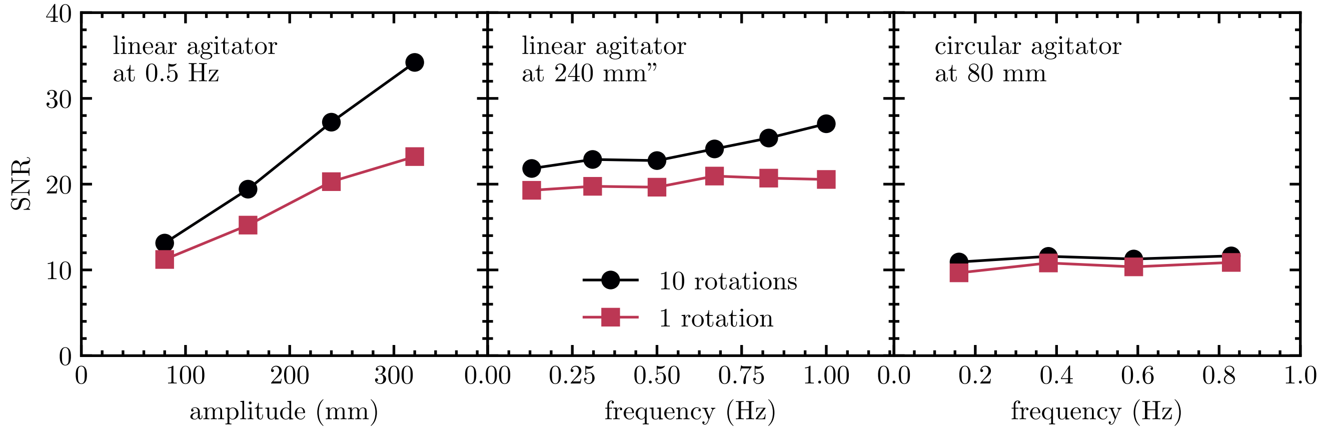

Fig. 6.— SNR comparison for varying amplitudes using the linear agitator (left) and varying frequencies using each of the linear (center) and circular (right) agitators. For the amplitude tests, the linear agitator was set at 0.5 Hz. For the linear agitator frequency test, the amplitude was set to 240 mm. The circular agitator can only be set to an amplitude of 80 mm. Integration times were set to match the period of 1 rotation (i.e. 2 s for 0.5 Hz agitation). The "10 rotations" data was calculated after co-adding 10 of these 1 rotation images. Results in the far field yielded similar correlations between amplitude, frequency, and SNR.

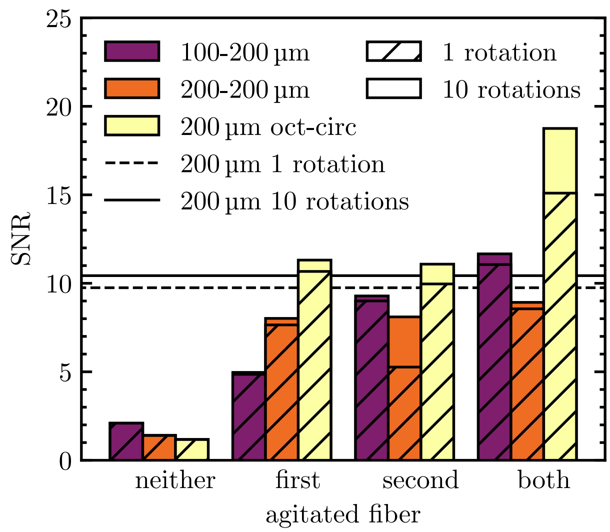

Fig. 7.— SNR for various arrangements of coupled fibers with varying core diameter and cross-sectional shape. All fibers are assumed to be circular unless otherwise stated on the plot. The SNR for a single 200 µm circular fiber is also presented for both 1 rotation (dashed) and 10 rotations (solid).

agitating a single 200 µm circular fiber. For this test fibers were agitated using the linear agitator at 80 mm and 1.0 Hz.

The results from these tests are shown in figure 7. For the most part, the SNR for each test hovers around 10, the same level at which the SNR would be for an uncoupled 200 µm fiber. However, the SNR when agitating only the 100 µm fiber is significantly less and the SNR when agitating both the coupled 200 µm octagonal and 200 µm circular fibers simultaneously is significantly more.

4.5. *Discussion*

Our results can be summarized as follows, the highest SNR is attained when a fiber has been put through as many physical configurations as possible over the length of an exposure. This is best accomplished using a coupled agitation setup comprised of, in our case, a linear and circular motion with the highest amplitude possible on each. One could conceive a random or chaotic agitator as a possible implementation. These conclusions are highly reminiscent of the idea that hand-agitation is consistently better than any form of mechanical agitation. Human motions are much less deterministic than a motor resulting in a more chaotic motion. Our combined linear/circular agitator with slightly different oscillation frequency mimics this behavior since it will chaotically reach many fiber configurations over a single calibration exposure of about 10 s. Note that the motion needs to be continuous to avoid build-up of a static speckle pattern within the exposure.

Our results indicate that large amplitude, relatively high frequency, chaotic coupled harmonic agitation for optical fibers that have large core cross-sectional area and low azimuthal symmetry yield the highest signal to noise. We therefore believe that the most important factor when agitating fibers is to place the fiber into as many physical configurations as possible over a single exposure., and can be done anywhere along the length of the fiber, allowing for large distance from a stabilized spectrograph.

We made this conclusion initially from the data present in figure 6 which shows a much stronger correlation between amplitude and SNR than between frequency and SNR. The data in figures 4 and 5 provide further evidence that placing the fiber into more physical configurations further increases the SNR.

Although most of the tests in this paper look at relatively low frequency agitation (i.e. less than 2 Hz), our conclusions support Plavchan et al. (2013) in that adding a high frequency "tweeter" is advantageous to reducing modal noise. This test showed significant improvements over high-amplitude with low-frequency, especially at longer exposures, and this appears to be because of this simultaneous high-frequency shaking placing the fiber into extra physical configurations.

5. RADIAL VELOCITY PRECISION

As discussed in section 2, optical fiber modal noise is an issue of centroid drift as well as diminished SNR. Therefore, we test our agitation method on the $100\,\mu\mathrm{m} \times 300\,\mu\mathrm{m}$ rectangular fiber over three hundred 1.0 s exposures to observe how the centroid drifts over time. The idealized method we use in this test includes the circular agitator oscillating at 1.1 Hz and the linear agitation set at 240 mm and 1.0 Hz. Keeping the two agitators at slightly different frequencies means that a large range of fiber configurations are reached after about 10 s. We compare this idealized method to a broadband light source (low modal noise) and a slowly agitated fiber (high modal noise). For the slow agitation test, we set only the linear agitator at 80 mm and 0.03 Hz meant to mimic the slight motions of the telescope throughout a night.

The results for these tests are shown in figure 8 where the RV error is calculated using equation 5. The dispersion direction for a rectangular fiber is along the short end, meaning that the diameter D is $100\,\mu\mathrm{m}$. The resolution is assumed to be 150,000, the current goal of EXPRES.

These results indicate that coupled agitation reduces errors induced by a slowly moving telescope by about three-fold and are minimized to about $37\,\mathrm{cm\,s^{-1}}$. This error is the RV error per line in the spectrograph, meaning that the total RV error after averaging over 30-40 lines would be significantly less than $10\,\mathrm{cm\,s^{-1}}$ [INSERT BETTER TOTAL RV ERROR HERE].

Using our prototype agitation setup in our lab, we were not able to reach the stability of continuum illumination ($9\,\mathrm{cm\,s^{-1}}$). However, we are confident that increasing the amplitude of circular motion, increasing the frequency of both agitators, and adding a "tweeter" element will continue to push this limit even lower.

6. CONCLUSIONS

We have tested a wide swath of agitation parameter space with the goal of further understanding the mechanism behind fiber agitation as a method for modal noise reduction.

The EXPRES fiber assembly will be employing the idealized agitation technique detailed in this paper. We will be combining a 160 mm amplitude circular and linear agitator similar to those seen in figure 2, but with greater stability to support an entire reinforced wrap of cables. The two agitators will oscillate at slightly different frequencies at the maximum speed deemed safe for the fibers. We will also include a large subwoofer speaker attached directly to the cable wrap to add simultaneous high frequency vibrations to the fibers.

The Fiber Characterization Station was built with support from the Fund for Astrophysical Research, Inc. Special thanks to Saki Kamon, Kristoffer Acuña, and Dominic Eggerman for their data-taking contributions to this project.

REFERENCES

Baudrand, J., & Walker, G. A. H. 2001, Publications of the Astronomical Society of the Pacific, 113, 851

Daino, B., De Marchis, G., & Piazzolla, S. 1980, Optica Acta: International Journal of Optics, 27, 1151

Epworth, R. 1978, in Fourth European Conference on Optical Communication (Genoa: Proceedings of the Fourth E.C.O.C, Genoa), 492–501

Fischer, D., Anglada-Escude, G., Arriagada, P., et al. 2016, PASP, 45

Halverson, S., Roy, A., Mahadevan, S., & Schwab, C. 2015, ApJ Letters, arXiv:1511.02856

Halverson, S., Mahadevan, S., Ramsey, L., et al. 2014, in Proc. SPIE, ed. S. K. Ramsay, I. S. McLean, & H. Takami, Vol. 9147, 1–6

Imai, M., & Asakura, T. 1979, Optics Communications, 30, 299

Jurgenson, C., Fischer, D., Mccracken, T., et al. 2016, in Proc. SPIE, Vol. 9908

Lemke, U., Corbett, J., Allington-Smith, J., & Murray, G. 2011, Monthly Notices of the Royal Astronomical Society, 417, 689

Mahadevan, S., Halverson, S., Ramsey, L., & Venditti, N. 2014, The Astrophysical Journal, 786, 1

McCoy, K. S., Ramsey, L., Mahadevan, S., Halverson, S., & Redman, S. L. 2012, in Proc. SPIE, ed. I. S. McLean & S. K. Ramsay, Vol. 8446, 8J 1–8

Nikitin, P. V., Stancil, D. D., & Erosheva, E. A. 2011, in IEEE Antennas and Propagation Society, AP-S International Symposium (Digest), Vol. 2, 1662–1665

Plavchan, P. P., Bottom, M., Gao, P., et al. 2013, in Proc. SPIE, ed. S. Shaklan, Vol. 8864, 0G 1–18

Redding, B., Popoff, S. M., & Cao, H. 2013, Optics Express, 21, 6584

Roy, A., Halverson, S., Mahadevan, S., & Ramsey, L. W. 2014, in Proc. SPIE, ed. S. K. Ramsay, I. S. McLean, & H. Takami, Vol. 9147, 1–7

Sablowski, D. P., Plüschke, D., Weber, M., Strassmeier, K. G., & Järvinen, A. 2015, Astron. Nachr., 1, 0

Stürmer, J., Schwab, C., Grimm, S., et al. 2016, in Proc. SPIE, ed. R. Navarro, Vol. 9912, 1T 1–7

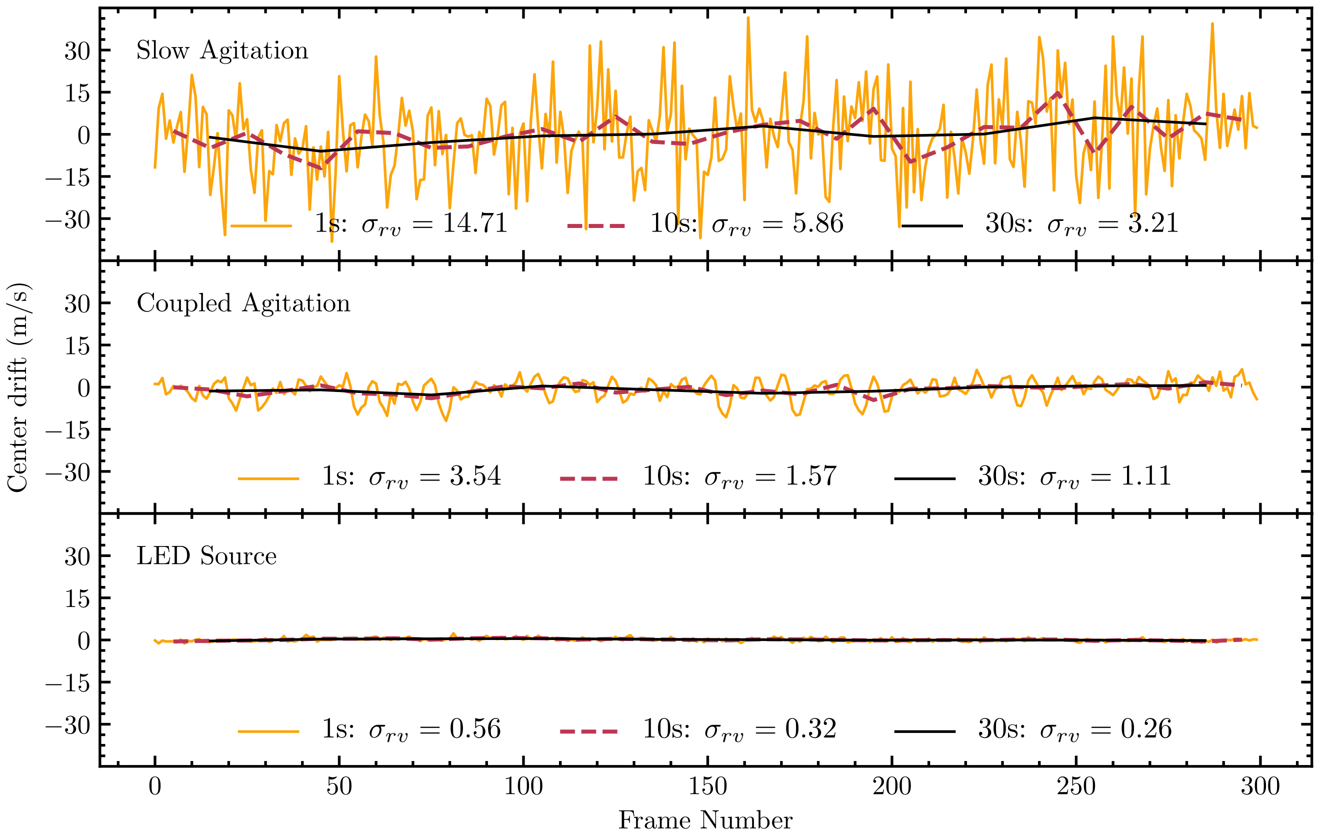

FIG. 8.— Centroid drift and resultant RV error for a slowly agitated fiber (top), coupled agitated fiber (middle), and LED illumination (bottom). The red line in each image is the 30-image average of these centroid drifts, effectively yielding the RV error for 30 second exposures. Note that the y-scales changes between the slow agitation and coupled agitation plots.